EFFECT OF WIND TUNNEL BLOCKAGE ON AERODYNAMICS OF CIRCULAR CYLINDERS

SAIB ABDULLA YOUSIF

Chemical Engineering Department, Engineering College,

Basrah University

E mail Saib60@yahoo.com

Abstract

Experimental investigation was conducted on low speed wind tunnel with (50 mm x100 mm) rectangular working section. Five smooth circular cylinders, as bluff bodies were applied. Cylinders diameters are 12.5, 15, 17, 35, and 37 mm which experience blockage ratio of 12.5%, 15%, 17%, 35%, and 37%, respectively. The range of Reynolds No. and air velocity for present study is $0.7 \times 10^4 - 5 \times 10^4$ and 10-20 m/s respectively which are more applicable in engineering field. The experiments were carried out in fluid mechanics laboratory, Faculty of engineering and technology, Sebha University, Libya. Results indicate that cylinders of blockage ratio of 35% and 37% experience lower pressure coefficients around bodies, lower velocity distribution in the wake, and higher drag coefficients. Drag coefficient correction is agreed with unconfined flow for blockage ratio less than 17%. Wake and buoyancy blockages may have effect on models of higher blockage ratios.

تأثير الانسداد في النفق الهوائي على الخصائص الايروديناميكية للأسطوانات الدائرية المقطع

صائب عبدالله يوسف

قسم الهندسة الكيمياوية، كلية الهندسة، جامعة البصرة

الخلاصة

اجريت دراسة عملية على نفق هوائي منخفض السرعة ذو مقطع اختبار مستطيل المقطع ابعاده 50 mm x 100 mm. استخدمت خمسة اسطوانات دائرية المقطع ناعمة السطح كنماذج. كانت اقطار الاسطوانات 12.5, 15, 17, 35, 37 mm مسببة نسبة انسداد 37%, 35%, 17%, 15%, 12.5% على التوالي. وكان حدود رقم رينولدز $0.7 \times 10^4 - 5 \times 10^4$ وحدود سرعة الهواء 10-20 m/s الاكثر تطبيقا في المجالات الهندسية. انجز الجانب العملي في مختبر ميكانيك الموائع، كلية العلوم الهندسية والتقنية، جامعة سبها، ليبيا. اثبتت الدراسة ان نسب الانسداد 37%, 35% سببت انخفاض معامل الضغط حول النماذج وانخفاض توزيع السرع في منطقة المخر (المنطقة الخلفية للاسطوانات) وزيادة معامل الاعاقة. تصحيح معامل الاعاقة كان متفقا مع معامل الاعاقة للجريان الغير محدد لنسب انسداد اقل من 17%.

Introduction

The purpose of wind tunnel is obtaining aerodynamics data such as, force and momentum coefficients, testing of different configurations, looking at high lift devices, reducing drag, and designing simulators before first flight. Unfortunately, the boundaries of wind tunnel test section impose constraints on the flow around bluff bodies which are even now not fully understood. The effects of the tunnel walls upon the flow over a model are separated in, solid blockage, streamline curvature, wake blockage, and buoyancy.

Marshell [1] devised one of the earliest blockage corrections for bluff bodies in a wind tunnel. From experience, Maskell, et. al. [2] shows that the limit of confident use of the Maskell scheme is about 10% blockage ratio. Several other blockage corrections have been devised (for example Castro [3], Allen, and Vincenli [4]), but all refer to uniform flow. West [5] concluded that for blockage ratio in the range 6-16%, there is considerable distortion of the flow and the effect is complex.

The aim of present work is to investigate the pressure distribution around model surface and velocity distribution in the wake at different blockage ratio up to 37%. However, corrected drag and pressure coefficients are aimed to be compared with uncorrected coefficients.

Theoretical Approach

Drag coefficient

Taking a control volume inside the working section of the tunnel, as shown in Fig. 1, the second moment of Newton law around model is,

$$2hp_s - 2hp_e - D = \int_{-h}^{h}\rho u^2 dy - \int_{-h}^{h}\rho U^2 dy \quad (1)$$

Where,

$2hp_s$; Upstream force per unit length of the model.

$2hp_e$; Downstream force per unit length of the model.

D; Drag force per unit length of the model.

$\int_{-h}^{h} \rho U^2 dy$; Moment rate at upstream of the model

$\int_{-h}^{h} \rho u^2 dy$; Moment rate at downstream of the model.

Dividing equation (1) by $\frac{1}{2}\rho U^2 d$ and rearranging, equation (1) becomes,

$$c_D = \frac{2h}{d}\frac{p_s - p_e}{\frac{1}{2}\rho U^2} + \frac{2}{d}\int_{-h}^{h}\left(1 - \frac{u^2}{U^2}\right)dy \quad --(2)$$

By using the definition of drag coefficient, $c_D = \dfrac{D}{\dfrac{1}{2}\rho U^2 d}$

y-coordinate is now made non-dimensional,

$$\eta = \frac{y}{h} \quad ----------- (3)$$

Thus,

$$\int_{-h}^{h}\left(1 - \frac{u^2}{U^2}\right)dy = h\int_{-1}^{1}\left(1 - \frac{u^2}{U^2}\right)d\eta$$

So,

$$c_D = \frac{2h}{d}\frac{p_s - p_e}{\frac{1}{2}\rho U^2} + \frac{2h}{d}\int_{-1}^{1}\left(1 - \frac{u^2}{U^2}\right)d\eta \quad (4)$$

Equation (4) is used to calculate drag coefficient from pressure drop through working section and velocity distribution at model wake. The contributions of both the pressure and friction are contained in drag force D. Equation (4) is fitted to flow through confined surface.

Corrected drag and pressure Coefficient

Drag and pressure coefficient are corrected experimentally based on the actual velocity U_1 in the gap between the model and tunnel wall which is measured by pitot tube located 3d downstream the model as shown in Fig. (2). the correction is,

$$c_{D_c} = \frac{D}{\frac{1}{2}\rho U_1^2 d} = \frac{D}{\frac{1}{2}\rho U^2 d}(\frac{U}{U_1})^2 \quad ---(5)$$

$$c_p = \frac{p - p_s}{\frac{1}{2}\rho U_1^2} = \frac{p - p_s}{\frac{1}{2}\rho U^2}(\frac{U}{U_1})^2 \quad -----(6)$$

Thus,

$$c_{D_c} = (\frac{U}{U_1})^2 c_D \text{ ----------- (7)}$$

And,

$$c_{P_c} = (\frac{U}{U_1})^2 c_p \text{ ----------- (8)}$$

While, Maskell correction formula [1] for the present flow range and with $\beta < 10\%$,

$$\frac{c_D}{c_{D_c}} = \frac{1}{1-1.5\beta} \text{ ---------- (9)}$$

Where, β is blockage ratio that is, projected area of the cylinder model to the cross sectional area of the empty working section.

Experimental Work

Fig. (2) is the schedule of wind tunnel used in present study. The air is propelled by a power driven fan (1). After passing the fan, the air travels along a duct (2) until it reaches a cascade of fixed vanes which deflect it through a right angle. On duct (2), there is a slide valve (3) for controlling air flow. It is now passed through a honeycomb whose function is to smooth the flow by breaking up large eddies. The air is now in the settling chamber (5), from which it passes to 50 mm x 100 mm rectangular working section (7) via a contraction (6). In the process of passing through the contraction the air is greatly speeded up while the flow is made smooth and regular. The working section has parallel walls and the velocity of the air here reaches its maximum. The downstream end of the working section is opened to atmosphere. Multi vertical manometers with liquid of specific gravity 0.784 and with scale calibrated in mbar are used to measure atmospheric, stagnation, and static pressures as shown in Fig. (2) and Fig. (3b). Stagnation pressure is measured in the settling chamber while static pressures are measured in the onset of the working section, around cylinder model surface, and in the wake at a distance 3d from the model. Five aluminum, smoothed circular cylinders of diameters 12.5, 15, 17, 35, and 37 mm are tested as bluff bodies

in the working section. The length of each cylinder is 48 mm. However, a hole of a diameter 1 mm is fabricated on a model surface to measure static surface pressure. The model is fixed in the tunnel wall by a screw, in between; there is a circular plate with angle scale. The plate may rotate to change the angle of surface hole 0^0-360^0. Pitot tube (8) located 3d downstream and perpendicular to the model plane is used to measure local velocities in the wake. The balance for measuring the forces on the models is situated outside the working section as shown in Fig. (3a), and is arranged to measure only drag force. Mercury thermometer (4) is located to measure surrounding temperature. Fig. (4) illustrates section in a model.

Results and Discussion

Velocity distribution at 3d downstream of the models with different blockage ratios is plotted in Fig. (5). There is obvious symmetry on both sides of the cylinders with lower velocity at the wake due to eddies formation. Once, pitot tube moves toward tunnel wall the velocity increases and becomes constant outside the wake at a value more than free stream velocity as a result of solid blockage effect. Since, according to continuity equation, when flow area decreases fluid velocity increases. At higher blockage ratio, e.g. 35% and 37%, the model exhibits lower velocity at the wake and experiences high momentum loss. Fig. (6) shows the drag force on the studied cylinders. The drag force is higher for high blockage ratio since the velocity through the gap between the model and tunnel wall is increased with blockage ratio causing the momentum to be increased as well. Pressure coefficient around model surface is studied as shown in Fig. (7).

6

When the air past the model, a boundary layer is formed over the cylinder surface and negative pressure gradient is created, $\partial p / \partial x < 0$. At approximately 75^0 the pressure gradient becomes positive which resists the flow and results in separation of boundary layer. Thus, as noted in Fig. (7), pressure coefficient is initially of value (1) at stagnation pressure in a point perpendicular to the flow. The pressure is then reduced gradually. After the angle 75^0, the pressure coefficient is oscillated at a certain value in the wake region due to eddies and swirls creation. Again, lower pressure coefficient is noted for higher blockage ratio resulting in higher form drag. When C_p is corrected based on velocity at actual flow area for two blockage ratios, e.g. 12.5% and 37%, the results is significantly improved as pointed out in Fig. (8) depending on actual free stream velocity. C_D is calculated from equation (4) by

using numerical integration to evaluate the second term. It is obvious from Fig. (9) that increasing of blockage ratio causes an increase of drag coefficient as a result of reduction of pressure coefficient and velocity in the wake region. The flow in present study is limited by the fan used. Thus, moderate flow with narrow range of Reynolds number is obtained. Generally, drag coefficient is relatively constant for unblocked flow and with Reynolds No. 10^4-10^5 [6,7]. Drag coefficient calculated in Fig. (9) is compared with that in unblocked state at different aspect ratios [6], e.g., dash and solid lines. There is discrepancy due to distortion of flow caused by end effect of the model and the effect of tunnel wall. The results are agreed with the work of West et. al. [5] at blockage ratio 12.5%. However, corrected C_D based on actual flow velocity is improved and there is an agreement for

blockage ratio less than 17% with that in unconfined flow [6] as reproduced in Fig. (10). Though there is an improvement of about 60% at high β, but still higher than that for unblocked flow. That is, due to wake blockage which may has genuine effect on large solid models [8]. The other effect is the buoyancy, the variation of the static pressure by thickening of the boundary layers along the tunnel walls, which increases with model size.

Conclusions

1. Solid blockage is considered in the present study.

2. Results indicate that cylinders of blockage ratio 35% and 37% experiences lower pressure coefficients around bodies, lower velocity distribution in the wake, and higher drag coefficients.

3. Drag coefficient is agreed well with the study of West et. al. [5] at blockage ratio 12.5%.

4. Corrected drag, pressure coefficients, and other aerodynamic properties are required for all above bodies.

5. Corrected C_D is improved by 60% but still higher than unconfined conditions for higher blockage ratio. This is due to increased interference between wall and model boundary layers. However, buoyancy and wake blockages may have significant effects at higher blockage ratio.

6. Maskell correction formula with β<10% is not fitted to present data.

7. Using large tunnel is not practical according to economical aspects. Thus, testing bluff bodies of blockage ratio less than 17% is recommended.

8. Empirical correlation relating corrected C_D with

Re, L/d, β, and parameters of buoyancy and wake blockages are recommended to get full similitude between model and prototype.

Nomenclature

A	Projected area of model, m^2
c_D	Drag coefficient.
c_{Dc}	Corrected drag coefficient.
c_p	Pressure coefficient.
c_{pc}	Corrected Pressure coefficient.
D	Drag force per unit length, N/m.
d	Cylinder diameter.
h	Half width of working section, m.
L	Model length, m.
p_e	Back (atmospheric) pressure, N/m^2.
p_o	Stagnation pressure, N/m^2.
p_s	Static pressure, N/m^2.
Re	Reynolds No.
U	Uniform free stream velocity, m/s.
u	Local velocity, m/s.
y	Horizontal distance along tunnel width, m.

References

[1] E. C., Maskell," A theory of the blockage effects on bluff bodies and stalled wings in a closed wind tunnel". ARC R. & M No. 3400, November, HMSO, 1963

[2] V. J., Modi, and S. E., El-sherbiny," Effect of wall confinement of an Aerodynamics of Stationary Circular Cylinders", 3rd International Conference of Wind Effects on Buildings and Structures, Saikon Shuppan CO., Ltd., Tokyo, Volume 2, pp. 365-376, 1971.

[3] F.P., Castro, and J.E., Fackrell, "A note on Two Dimensional Fence Flows with Emphasis on Wall Constraint", J. Industr. Aerodynamics, 3(1), March 1978.

[4] H.J., Allen, and W.G., Vincenti," Wall Interference in a Two-Dimensional Flow Wind

Tunnel, NASA Report No.782, 1944.

[5] G. S., West, and C. J., Apelt, "The Effect of Tunnel Blockage and Aspect Ratio on the Mean Flow Past a Circular Cylinder with Reynolds Numbers Between 10^4 and 10^5," J. Fluid Mech., 114, pp. 361-377, 1982.

[6] J.W., Daily, and R.F., Harleman, "Fluid Mechanics", Addison-Wesley Press, USA, (1966).

[7] J.F., Douglas, J.M., Gsiorek, and J.A Swasfield, "Fluid Mechanics", 3rd Edition, Longman Press, U.K., 1998.

[8] R.W., Gould, "Wake Blockage Corrections in a Closed Wind Tunnel for One or Two wall-mounted Models Subjected to Separated Flow", ARC R&M No. 3649, 1970.

Tunnel, NASA Report No.782, 1944.

[5] G. S., West, and C. J., Apelt, "The Effect of Tunnel Blockage and Aspect Ratio on the Mean Flow Past a Circular Cylinder with Reynolds Numbers Between 10^4 and 10^5," J. Fluid Mech., 114, pp. 361-377, 1982.

[6] J.W., Daily, and R.F., Harleman, "Fluid Mechanics", Addison-Wesley Press, USA, (1966).

[7] J.F., Douglas, J.M., Gsiorek, and J.A Swasfield, "Fluid Mechanics", 3rd Edition, Longman Press, U.K., 1998.

[8] R.W., Gould, "Wake Blockage Corrections in a Closed Wind Tunnel for One or Two wall-mounted Models Subjected to Separated Flow", ARC R&M No. 3649, 1970.

10
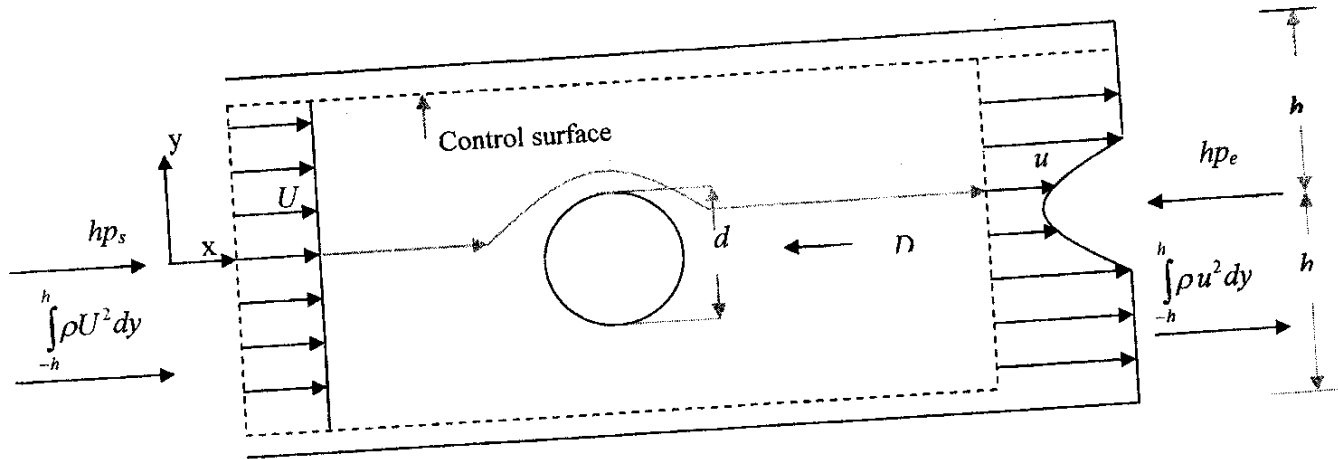
Fig. 1. Control Volume in the Working Section
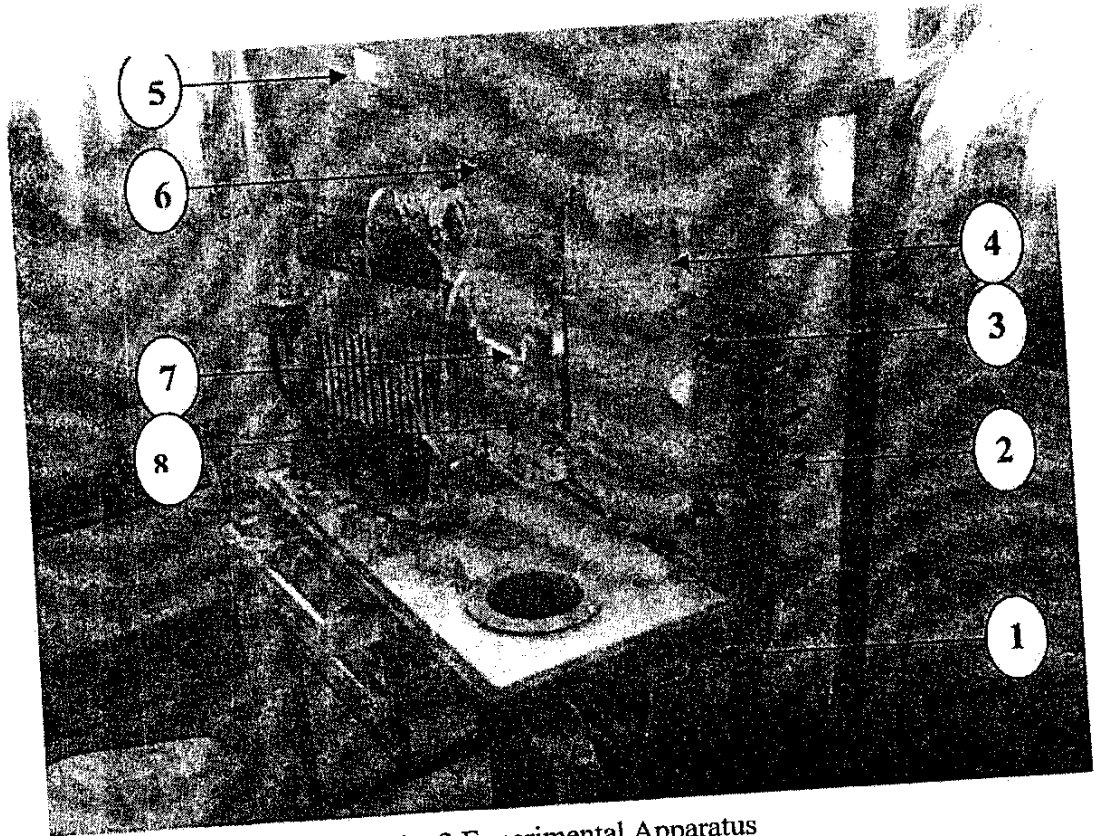
Fig. 2.Experimental Apparatus
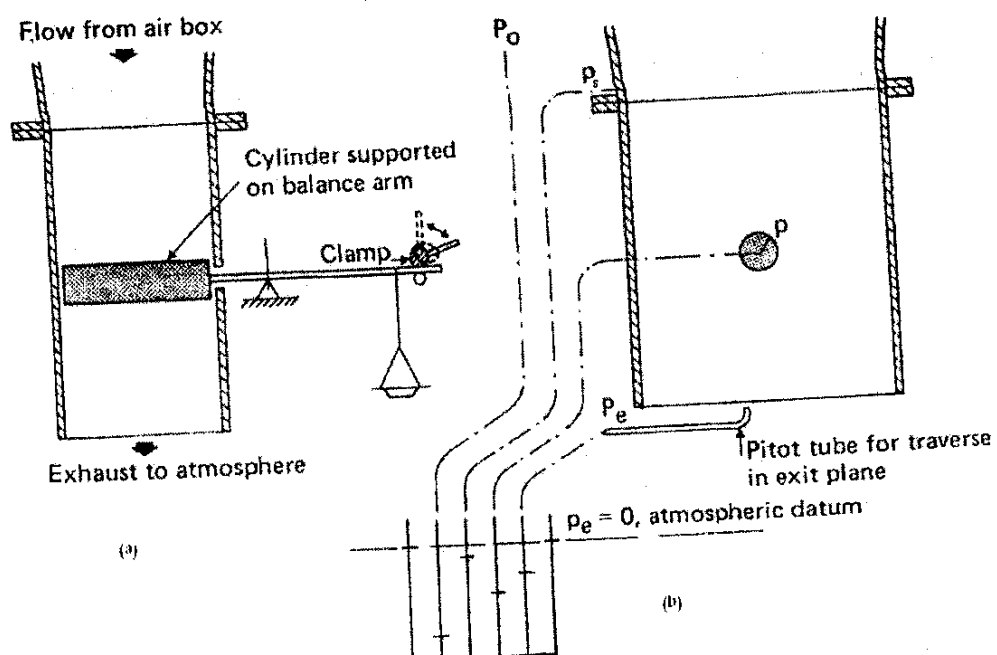
Fig. 3. a- Connection of balance to the cylinder. b- Manometers arrangement.
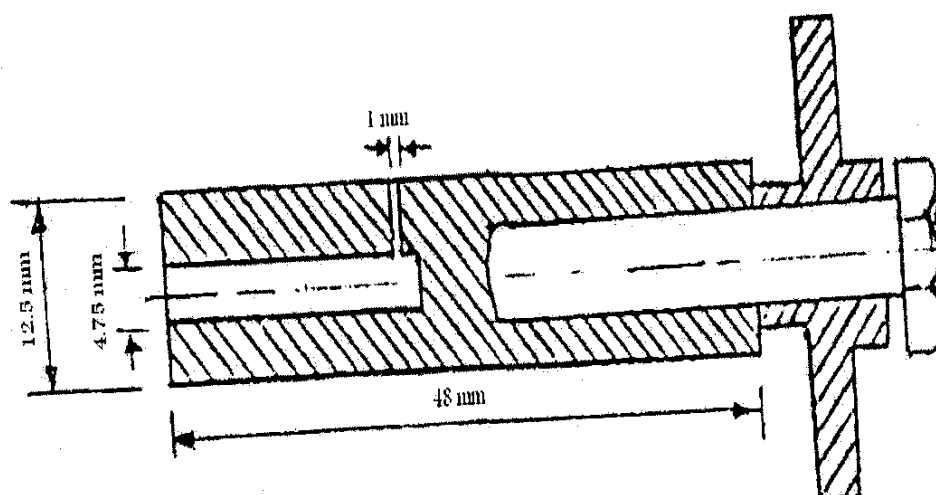
Fig. 4. Cylinder Model Section.

12
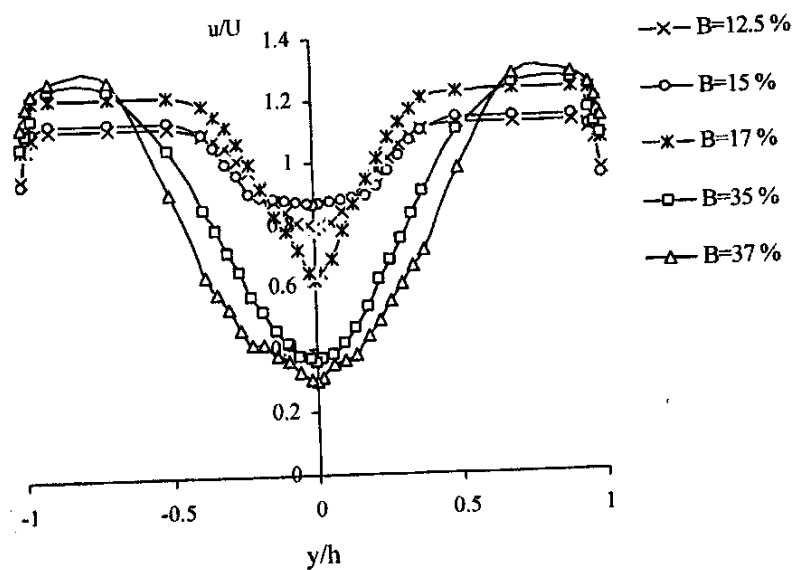
Fig. 5. Velocity distribution at the wake for air velocity 20 m/s
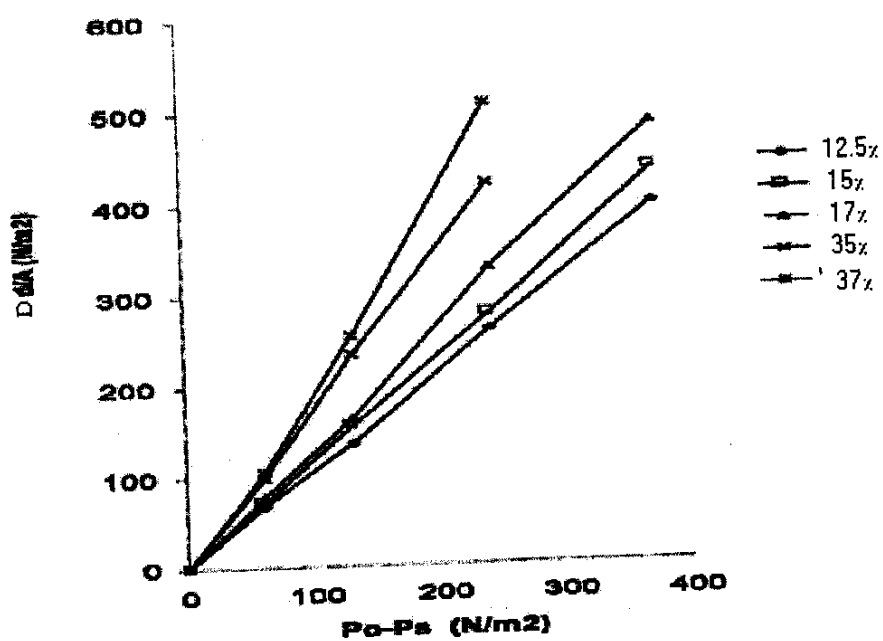

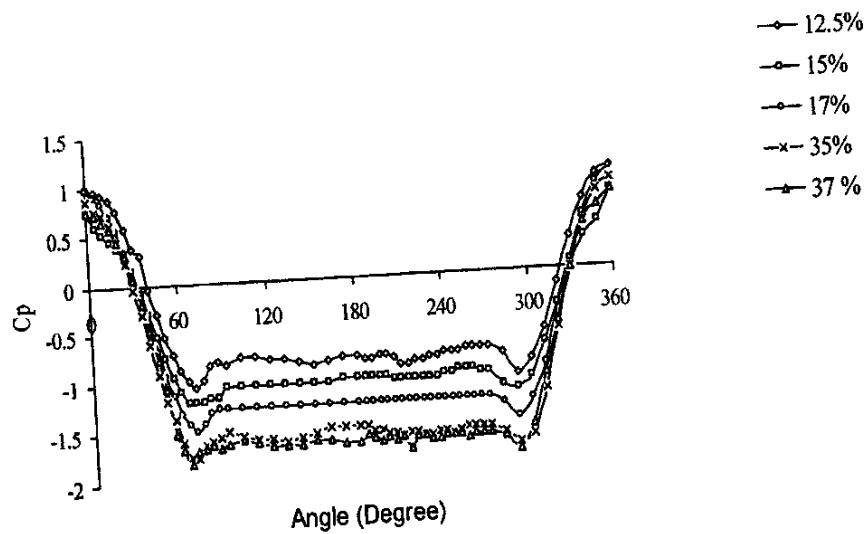Fig. 6. Drag force versus dynamic pressure at different blockage ratios.

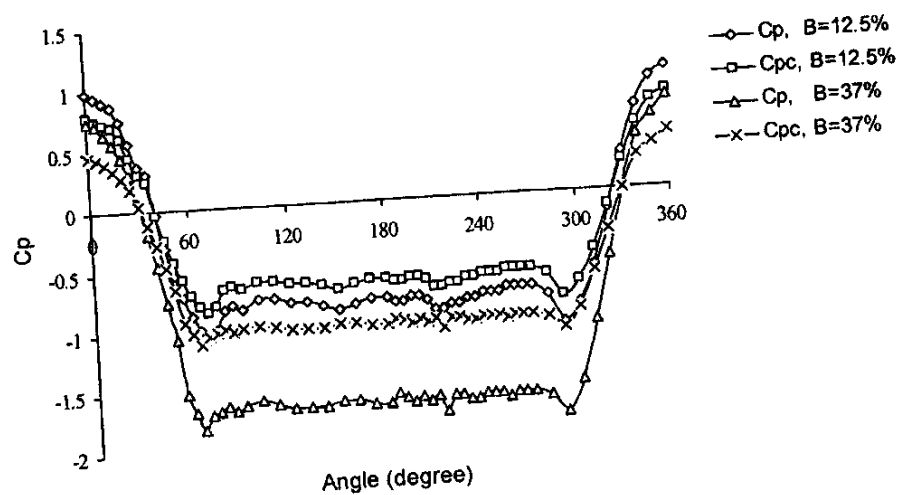Fig. 7. Pressure coefficient versus angle at air velocity 20 with different blockage ratios.

Fig. 8. Pressure and Corrected pressure coefficient versus angle at air velocity 20 m/s
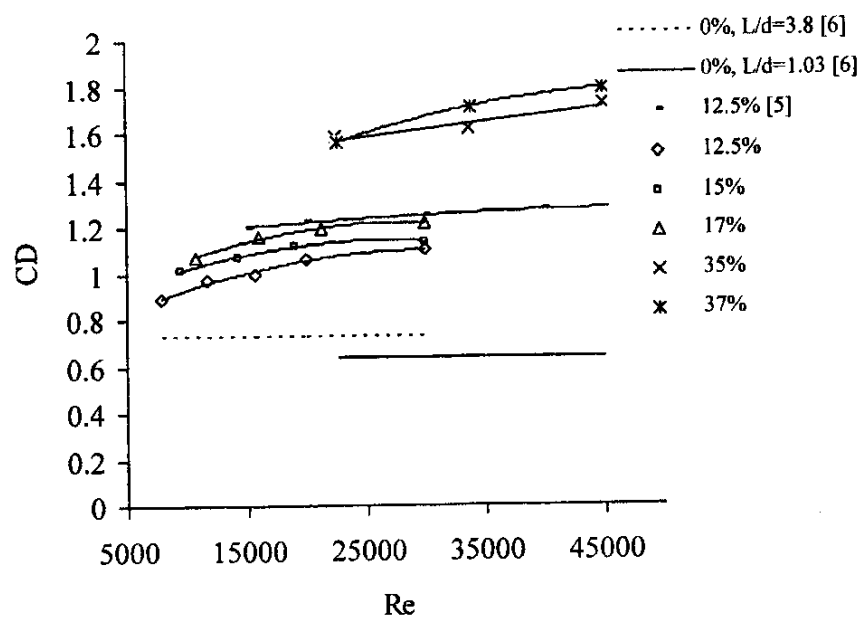
Fig. 9. Uncorrected drag coefficient with Reynolds No. at different blockage ratios.
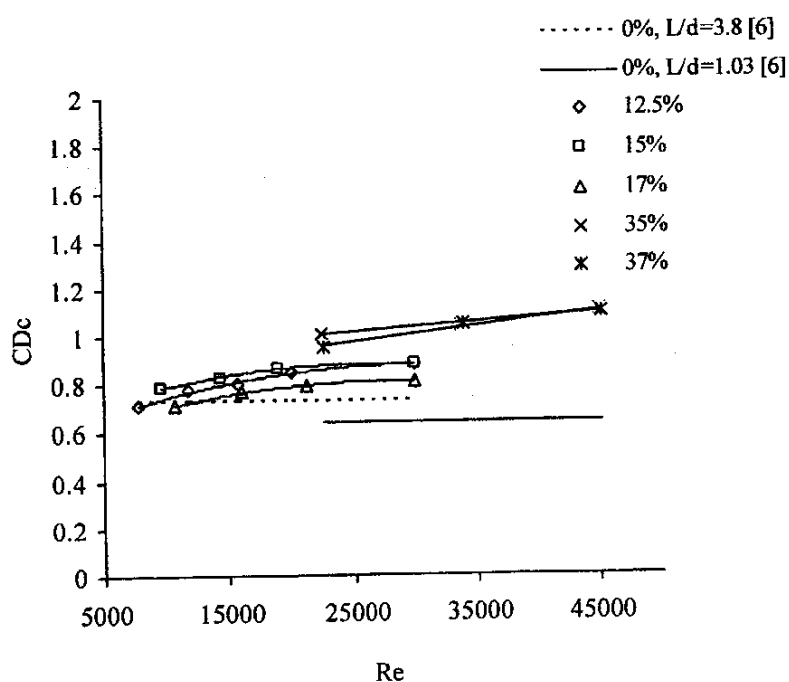

Fig. 10. Corrected drag coefficient with Reynolds No. at different blockage ratios.